ACCOUNTS
of chemical research

Probing Single Biomolecules in Solution Using the Anti-Brownian Electrokinetic (ABEL) Trap

QUAN WANG,[†,‡] RANDALL H. GOLDSMITH,[†,⊥] YAN JIANG,[†,§] SAMUEL D. BOCKENHAUER,[†,∥] AND W.E. MOERNER*[,†]

[†]*Department of Chemistry,* [‡]*Department of Electrical Engineering,* [§]*Department of Applied Physics,* [∥]*Department of Physics, Stanford University, Stanford, California, United States*

RECEIVED ON NOVEMBER 23, 2011

CONSPECTUS

Single-molecule fluorescence measurements allow researchers to study asynchronous dynamics and expose molecule-to-molecule structural and behavioral diversity, which contributes to the understanding of biological macromolecules. To provide measurements that are most consistent with the native environment of biomolecules, researchers would like to conduct these measurements in the solution phase if possible. However, diffusion typically limits the observation time to approximately 1 ms in many solution-phase single-molecule assays. Although surface immobilization is widely used to address this problem, this process can perturb the system being studied and contribute to the observed heterogeneity.

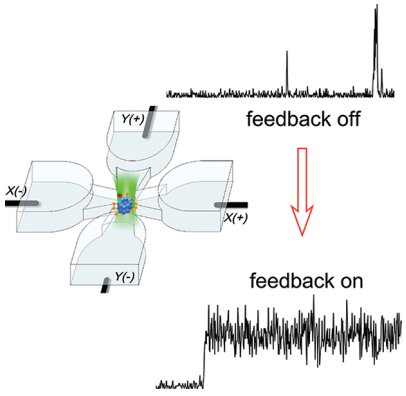

Combining the technical capabilities of high-sensitivity single-molecule fluorescence microscopy, real-time feedback control and electrokinetic flow in a microfluidic chamber, we have developed a device called the anti-Brownian electrokinetic (ABEL) trap to significantly prolong the observation time of single biomolecules in solution. We have applied the ABEL trap method to explore the photodynamics and enzymatic properties of a variety of biomolecules in aqueous solution and present four examples: the photosynthetic antenna allophycocyanin, the chaperonin enzyme TRiC, a G protein-coupled receptor protein, and the blue nitrite reductase redox enzyme. These examples illustrate the breadth and depth of information which we can extract in studies of single biomolecules with the ABEL trap.

When confined in the ABEL trap, the photosynthetic antenna protein allophycocyanin exhibits rich dynamics both in its emission brightness and its excited state lifetime. As each molecule discontinuously converts from one emission/lifetime level to another in a primarily correlated way, it undergoes a series of state changes.

We studied the ATP binding stoichiometry of the multi-subunit chaperonin enzyme TRiC in the ABEL trap by counting the number of hydrolyzed Cy3-ATP using stepwise photobleaching. Unlike ensemble measurements, the observed ATP number distributions depart from the standard cooperativity models.

Single copies of detergent-stabilized G protein-coupled receptor proteins labeled with a reporter fluorophore also show discontinuous changes in emission brightness and lifetime, but the various states visited by the single molecules are broadly distributed. As an agonist binds, the distributions shift slightly toward a more rigid conformation of the protein.

By recording the emission of a reporter fluorophore which is quenched by reduction of a nearby type I Cu center, we probed the enzymatic cycle of the redox enzyme nitrate reductase. We determined the rate constants of a model of the underlying kinetics through an analysis of the dwell times of the high/low intensity levels of the fluorophore versus nitrite concentration.

Introduction

Since the early advances in low temperature optical detection of individual molecules in the condensed phase,[1−3] single-molecule (SM) spectroscopy has evolved to become a powerful method to probe spatial-temporal inhomogeneity and asynchronous dynamics in a variety of scientific disciplines. One area of particular recent interest involves the single-molecule biophysics of proteins, enzymes, and oligonucleotides. Detailed mechanisms of DNA processing,[4] protein conformational dynamics,[5] enzymes,[6,7] molecular

Published on the Web 05/22/2012 www.pubs.acs.org/accounts
10.1021/ar200304t

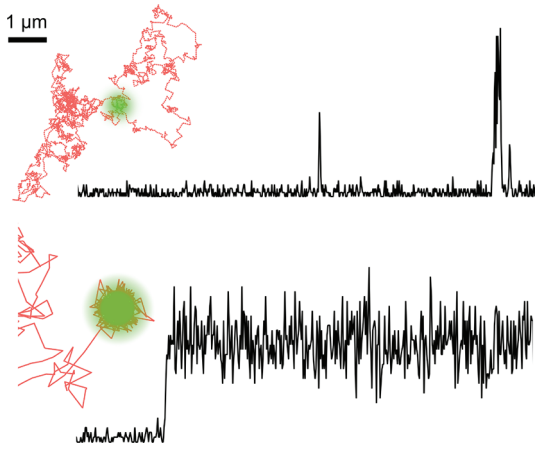

FIGURE 1. In conventional solution-phase single-molecule detection methods (top), the observation window is limited by diffusion to about 1 ms. The intensity observed on a photon detector (black trace) is not a good measure of the brightness of the object due to the inhomogeneous Gaussian profile of a focused laser beam (green spot) and the randomness of the trajectory (red). The ABEL trap (bottom) approximately cancels Brownian motion by real-time feedback, allowing molecules to be interrogated for seconds (red trajectory ending at the green excitation spot), limited mostly only by photobleaching. Careful design of the excitation optics creates a time-averaged flat-top profile. The brightness of the object can be reliably inferred from the intensity traces (black trace).

motors,[8] and many other biomolecular processes have been extracted from single-molecule studies.[9−12]

Most biological processes take place in an aqueous-like environment. However, single-molecule spectroscopy in solution faces an interesting dilemma: in order to increase the signal-to-background ratio, a tightly focused confocal geometry has to be used,[13] but the molecule easily escapes the diffraction-limited focal volume (∼1 fL) due to the perpetual thermal agitation from surrounding solvent molecules under ambient conditions. As a direct consequence of this intrinsic jiggling of the molecules, the observation time of single molecules in solution by methods such as fluorescence correlation spectroscopy (FCS) has been limited to about 1 ms. Nevertheless, FCS can extract much information about stationary short-time temporal fluctuations arising from molecular dynamics.[14,15] At the same time, due to the randomness of Brownian motion and the nonuniformity of the Gaussian profile of the focused spot, the brightness of each SM is poorly defined. Sophisticated statistical methods such as the photon counting histogram,[16] which essentially average among different single molecules, have to be used to study brightness changes and/or distributions.

In an alternate approach, individual enzyme molecules or proteins can be immobilized or encapsulated by various means.[17] In the case of enzymes, data can be acquired for many catalytic cycle turnovers, allowing statistically robust conclusions to be drawn regarding the extracted rate constants, but there are still a range of situations where immobilization or surface attachment may be deleterious.[18]

To overcome these limitations, we have developed a microfluidic-based experimental platform called the anti-Brownian electrokinetic trap (ABEL) trap,[19] which enables prolonged observation (∼seconds) of biomolecules in solution without surface immobilization (Figure 1). In this Account, we describe our recent advances in using this device to study biomolecules. We first briefly outline the working principle of the ABEL trap and provide four examples of applying the trap to uncover new physical insight: photophysical dynamics of the photosynthetic antenna allophycocyanin, sensing of cooperativity in a multi-subunit chaperonin enzyme TRiC, conformational dynamics of G protein-coupled receptors, and redox cycling of the enzyme nitrite reductase.

Working Principles of the ABEL Trap

The basic idea of the ABEL trap is remarkably simple: we continuously track the spatial position of the molecule, calculate its Brownian displacement from a trap center, and manipulate the molecule back to the center by electrokinetic forces. Two critical components enable the ABEL trap: microfluidic feedback actuation and real-time position tracking.

Trapping experiments are carried out in a microfluidic cell, made entirely of fused silica[20] or of PDMS[21] on top of a glass coverslip (Figure 2c). The center region of the cell holds the liquid sample in a thin sheet with dimensions of 20 μm × 20 μm (in x−y) × 0.6 μm (in z). The current implementation of the ABEL trap counters Brownian motion in the x−y plane and diffusion in z is confined by the top and bottom walls of the cell; future designs can trap in three spatial dimensions as well. Feedback manipulation is achieved by 2D electrokinetic forces as follows. For charged molecules, voltages applied on macroscopic electrodes inserted into the trapping cell are used to create electric fields and electrophoretic motion. On the other hand, confinement in the z direction helps support strong electroosmotic flows in the presence of mobile surface counterions, making the apparatus equally capable of trapping objects that do not carry net charges.

The more challenging task of the ABEL trap is to promptly estimate the position of nanosized objects with high bandwidth. To be trapped, biomolecules have been chosen to be fluorescent, either intrinsically or externally modified with probes. The initial incarnation of the trap used a high

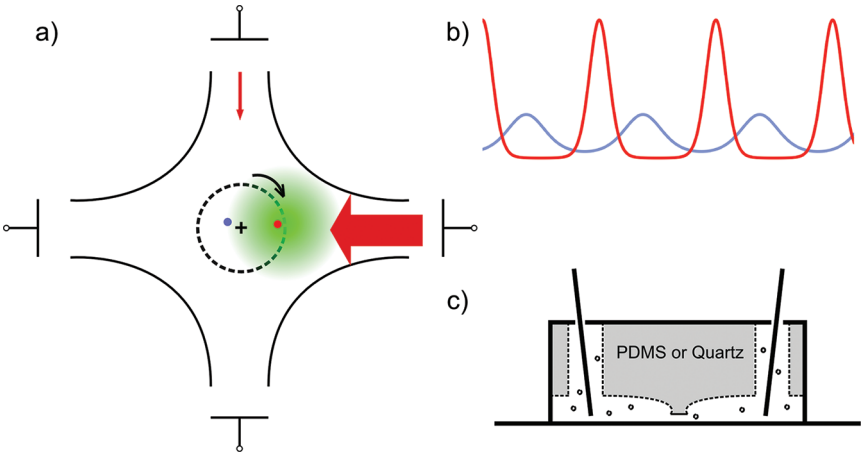

FIGURE 2. Position sensing and microfluidic feedback of the revolving-beam ABEL trap: (a) The excitation laser spot revolves around the trap center (black cross), generating a time-dependent intensity. The same object, when at different positions (red and blue dots in a), produces a differently modulated fluorescence signal (b, red and blue). The position of the object can be estimated by analyzing the amplitude and phase of the fluorescence signal. Feedback forces are then applied to the microfluidic environment accordingly (red arrows) to cancel Brownian displacements. (c) Side schematic view of the microfluidic cell along one dimension with inserted electrodes.

sensitivity camera to localize the molecule by centroid fitting of its fluorescent image,[19,22] but the delay time (~4 ms) introduced by image acquisition and processing was too high to trap molecules smaller than 20 nm in diameter. To go faster, a modulation/demodulation scheme was adopted to provide position estimates with a delay as short as 25 μs.[20] This scheme, originally proposed by Enderlein,[23] and later implemented in tracking systems by the Gratton[24] and Mabuchi laboratories,[25,26] uses a high-speed revolving excitation beam to modulate the fluorescence emission rate of the molecule. In this way, radial distance information is encoded on the *amplitude* of the fluorescence signal at the modulation frequency, while the azimuth angle of displacement can be retrieved by analyzing the *phase* of the modulated fluorescence with respect to the revolving beam (Figure 2b). Thus, by demodulation of the detected fluorescence signal, the coordinates of the molecule can be estimated with high bandwidth without the use of a camera. Another advantage of using a photon-counting avalanche photodiode instead of a camera is the ability to time tag each detected photon with high timing resolution (~300 ps). This revolving beam algorithm, first implemented with an analogue circuit[22] and later on a field-programmable-gate-array (FPGA) platform,[27] has enabled trapping and interrogation of a variety of biomolecules, including those described in this Account.

Recent technical improvements of the ABEL trap have focused on optimizing the real-time position estimation algorithm. Since fluorescently labeled biomolecules are generally dim (<20 000 detected photons/s) and diffuse quickly (diffusion coefficient $D > 40$ μm^2/s), the demodulation algorithm is usually configured with minimal integration time, in order to minimize feedback delay. In this regime, at most one or a few photons are detected each integration period, from which only the azimuthal angle of the molecule can be estimated. More optimal beam scanning patterns have since been proposed and implemented,[28,29] allowing position information to be directly extracted from every detected photon. These new scanning schemes have enabled use of the Kalman filter, a well-known algorithm in the engineering community, to make optimal feedback decisions based on a priori knowledge of measurement uncertainty and system dynamics. The newer generations of the ABEL trap have recently been used to trap single-stranded DNA fragments[30] and extremely bright and stable single fluorophores[31] with the added capability to measure the diffusion coefficient and electrokinetic mobility of trapped objects, even in real-time. We turn now to example applications of the ABEL trap.

Photophysical and Conformational Dynamics of Allophycocyanin

Photosynthetic antenna proteins are responsible for harvesting excitons from incident light and shuttling those excitons to reaction centers where charge separation and subsequent chemical reactions utilize the light's energy for organism function.[32] Antenna proteins represent highly optimized systems, where the precise arrangement and orientation of nonpeptide chromophore units are critical to the protein's performance. Consequently, study of antenna

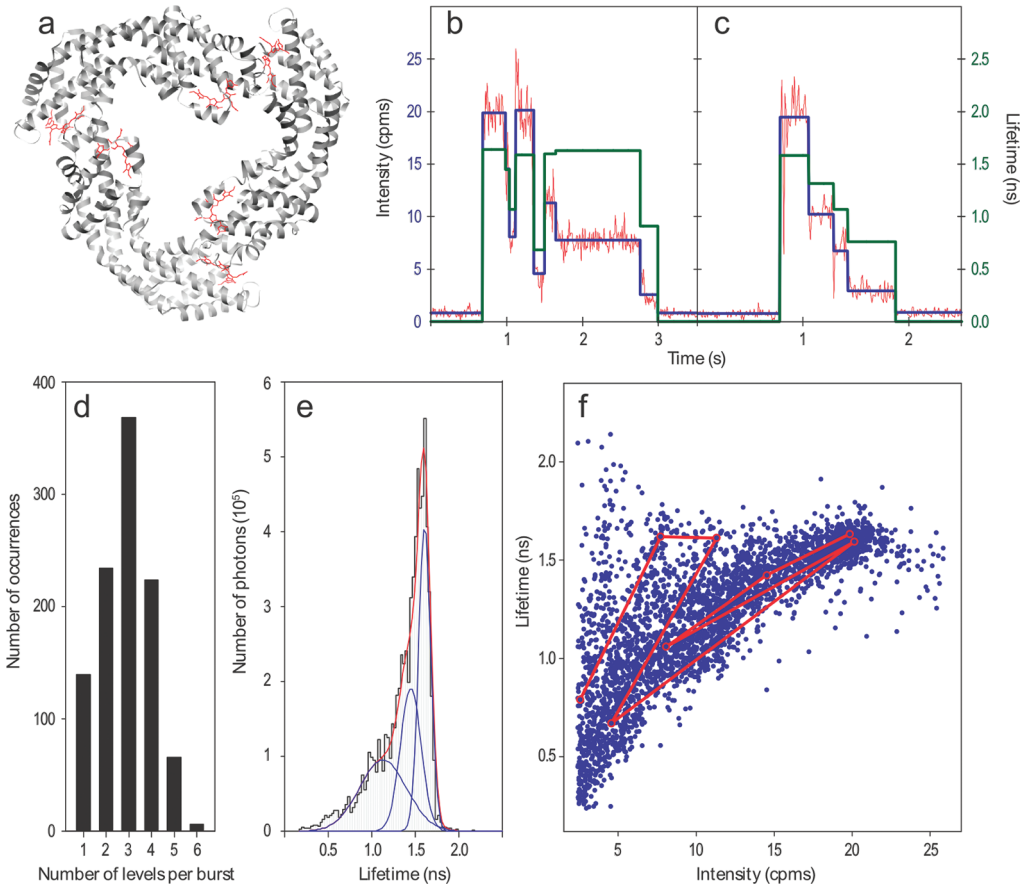

FIGURE 3. Photodynamics of single allophycocyanin (APC). (a) Each molecule of APC contains three pairs of phycocyanobilin chromophores (red). (b,c) Individual molecules of solution-phase APC exhibit shifts between distinct intensity levels (blue and red traces, left axis) as well as fluctuations of fluorescence lifetime (green trace, right axis), that may or may not be correlated with the intensity shifts. (d) Multiple intensity levels, up to four or more, are typically seen in each molecule. (e) A distribution of fluorescence lifetimes was measured, with a narrow central peak and a broad shoulder at shorter lifetimes, shown with a three-Gaussian fit. (f) Single intervals can be characterized by a single intensity and lifetime (blue circles). APC molecules typically initially exhibit a narrow distribution of high intensities and long lifetimes, but after repeated photoexcitation display a broader distribution of intensities and shorter lifetimes (red trace, corresponding to the dynamics shown in panel b)).

proteins without significant perturbation of the protein matrix responsible for maintaining the orientation of the chromophores is extremely desirable.

Allophycocyanin (APC, Figure 3a) is a photosynthetic antenna protein found in red algae and cyanobacteria where it is an important component of the phycobilisome exciton funnel.[33] The photophysical properties of APC are dominated by six covalently bound phycocyanobilin (PCB) molecular cofactors that form three pairs at the interfaces between the three protein monomers upon fulfillment of the protein's native quaternary structure.[33]

Single molecules of APC, upon diffusion into the excitation volume, are localized at the center of the ABEL trap and experience spatially flat excitation from the rapidly revolving laser spot.[34] Once in the trap, clear stepwise intensity changes, Figure 3 (b and c), arise primarily from molecular photodynamics, as opposed to the case with FCS where the molecule diffuses in a nonuniform Gaussian spot. To count the number of intensity levels per APC, we employed a change-point-finding algorithm[35] which yields the blue traces in Figure 3 (b and c). A histogram of the number of distinct brightness levels identified from each APC molecule is shown in Figure 3d, and many individual molecules demonstrate four or more unique levels. This result parallels that for APC immobilized in PVA[36] but contrasts with APC immobilized in agarose or on glass[37] and suggests that some immobilization environments may cause APC to deviate from its solution-phase behavior.

Time-stamping of recorded photons relative to each excitation pulse opens a second channel for observing the dynamics of solution-phase fluorescent proteins.[38] Histogramming pump-detect delay times from photons collected over a given intensity interval allows determination of the time-varying fluorescence lifetime, green traces in

Figure 3 (b and c).[34] A highly asymmetric fluorescence lifetime histogram is shown in Figure 3e. The highest peak has a 75% smaller width than that for the analogous peak for APC trapped in PVA.[36] This reduction implies that immobilization contributes to inhomogeneous broadening of APC's lifetime and that these effects are suppressed here.

Simultaneous measurement of fluorescence lifetime and intensity of individual solution-phase APC molecules provides a revealing window into the photo- and conformational dynamics of these proteins.[34] Figure 3f plots for each intensity interval the average intensity versus the determined fluorescence lifetime for 1048 individual APC molecules. Each marker indicates one point in the intensity-lifetime trajectory of one APC molecule. Upon first entering the ABEL trap, most APC molecules belong to a relatively homogeneous population with high intensity (~20 cpms) and narrow lifetime distribution (~1.5 ns), upper right of Figure 3f. Only after repeated photoexcitation do molecules shift to dimmer states with larger lifetime distributions, implying photoinduced dynamics.

Fluctuations in lifetime and intensity are usually correlated, but are sometimes uncorrelated or anticorrelated. The correlated changes can be understood as stemming from the creation of nonemissive radical cation quenching centers[34] which induce protein matrix conformational fluctuations. Alternatively, dissipation of excess vibronic energy has also been shown to cause protein conformational changes.[39] Unexpectedly, these changes cause fluctuations of the PCB chromophore's radiative lifetime, as evidenced by observed shifts in fluorescence lifetime at *constant* intensity[40] as a result of prolonged photoexcitation. While APC is frequently quenched in vivo via the other phycobiliproteins in the phycobilisome, these photoinduced changes may represent dire consequences for the organism under conditions of high fluence, and necessitate photoprotection mechanisms. By providing a new way of probing solution-phase protein dynamics, the ABEL trap revealed previously hidden photodynamics at the single-molecule level.

Studying Cooperativity in Multi-Subunit Enzymes

Many vital proteins in living organisms are multi-subunit complexes, such as hemoglobin, proteasomes, some chaperones, to name a few. In these proteins, cooperative interactions are critical for the subunits to work in a coordinated fashion.[41−43] Cooperative processes often appear extraordinarily complicated due to the heterogeneity in the states of the subunits in various copies of the biomolecule.[44]

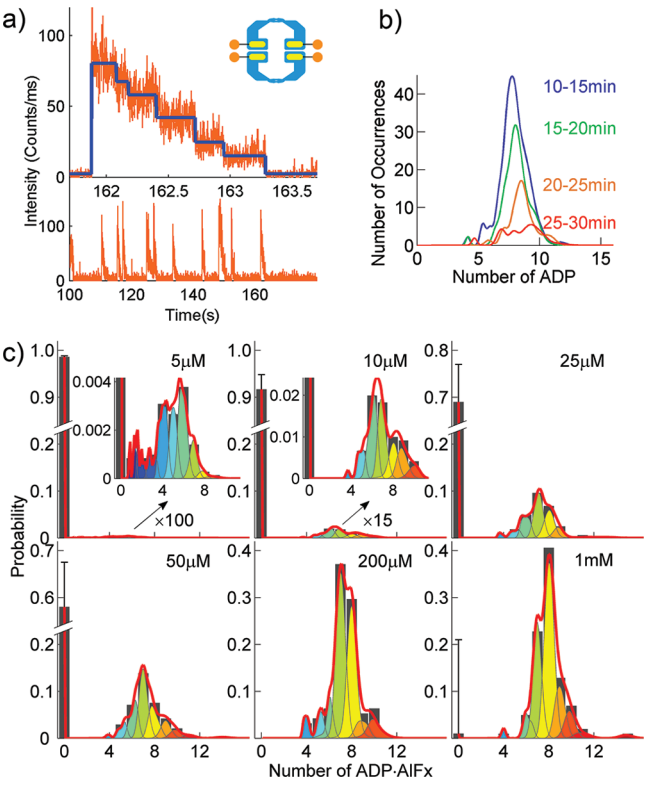

FIGURE 4. Experimental design and example data. (a) Fluorescence signal from Cy3-ADP showing individual trapped TRiC with several bound nucleotides (inset) entering the trap and photobleaching (lower) and expansion of the time axis for one of the events (upper). Blue line: the steps found by the change-point-finding algorithm[35,50] reflecting the photobleaching of individual Cy3. (b) Distribution of Cy3-ADP number on each TRiC as a function of time for the sample without AlFx. (c) Hydrolyzed ATP number probability distributions at six different incubation [ATP] for the sample with AlFx. Black bars (partially blocked by the colored areas): histograms of the calculated integer number for every complex. Colored areas: probability distributions of the actual ADP·AlFx number for the complexes grouped in each gray bar. Red curve: the total probability distribution of the ADP·AlFx numbers. Error bar: the uncertainty of the measured probability of TRiC with no ADP·AlFx, determined using the separate Atto647 label.

With the ABEL trap, cooperativity in a mammalian group II chaperonin TRiC/CCT has been studied in aqueous buffer.[45] TRiC has two ring-shaped cavities with built-in lids composed of eight different subunits each and is essential for the folding of a number of key proteins in mammalian cells, including actin, tubulin, and many cell cycle regulators.[46] Each of the 16 subunits in TRiC can bind and hydrolyze ATP. Binding and hydrolysis of ATP induces the conformational change between open and closed cavities, which is required for TRiC to bind and fold substrates.[47] Previous ensemble measurements show evidence for positive and negative cooperativity during the ATPase cycle,[48,49] but to access the molecular details of the cooperativity

single-molecule experiments in the ABEL trap were performed.[45]

The experiment consists of incubating with fluorescent Cy3-labeled ATP, allowing hydrolysis to occur, and directly counting the number of nucleotides found on each copy of TRiC (Figure 4a, inset). This yields the hydrolyzed ATP number distribution, which may be interpreted as the probability of having a particular number of hydrolyzed ATP present on a single enzyme chosen at random. As shown in Figure 4a, individual trapped TRiC show stepwise decreasing fluorescence intensity traces, due to the photobleaching of individual Cy3 dyes. Analysis of the traces allows measurement of number of nucleotides bound to each chaperonin; repeating for many copies yields a nucleotide number distribution.

One set of measurements[45] consisted of TRiC/Cy3-ADP complexes which were followed in time to measure the time-dependent ADP release process (Figure 4b). Since released Cy3-ADP diffuses quickly and is not trapped, the observed number distribution counts the Cy3-ADP which remained bound on the chaperonin. While the size of the peak decreases over time, the position stays around eight, indicating that all eight ADP molecules are released simultaneously. This striking behavior clearly reveals that ADP release by TRiC is a highly cooperative process, which would be difficult to detect by ensemble-averaged measurements.

Incubation with Cy3-ATP and AlFx produced stable Atto647-TRiC/Cy3-ADP·AlFx complexes locked at the transition state of hydrolysis. Distributions of the number of Cy3-ADP·AlFx on each chaperonin were obtained for various incubation ATP concentrations [ATP] (Figure 4c). Surprisingly, although there are 16 binding pockets available, each TRiC hydrolyzes only eight ATP even at saturating [ATP] (1 mM). Moreover, except for [ATP] $< 25\ \mu$M, TRiC hydrolyzes either eight ATP or essentially none at all. Like the previous ensemble measurements, the ensemble average of the single-molecule data can be matched with standard models.[41−43] However, the distributions themselves depart from standard models,[45] illustrating the power of the ABEL trap in discovering new phenomena and constraining cooperativity models for the chaperonin TRiC. With properly labeled fluorescent ATP or other substrates, this ability can be easily extended to other multi-subunit enzymes.

Conformational Dynamics of G Protein-Coupled Receptors

It is also possible to use a single fluorescent label as both a trapping dye and a reporter of conformational dynamics in an otherwise nonfluorescent protein. This concept was applied to probe conformational states and dynamics of the β_2-adrenergic receptor (β_2AR), a model member of the G protein-coupled receptor (GPCR) class of proteins, in the absence and presence of agonist.[27,51]

GPCRs comprise a large class of seven-helix transmembrane (TM) proteins which regulate cellular signaling by sensing light, ligands, and binding proteins.[52] The GPCR signaling process, however, is not a simple on−off switch;[53] current models suggest a complex conformational landscape in which the active, signaling state includes multiple conformations with similar downstream activity, ultimately regulating a broad range of important physiological processes.[54] Although crystal structures of agonist-bound β_2AR are now available,[55] these can provide only a snapshot of conformation in the stable, crystallized state. To probe the time scales of conformational interconversion in β_2AR, the cytosolic end of the TM6 helix was labeled with the environment-sensitive dye tetramethylrhodamine (TMR).[27] Bulk spectroscopy showed a significant increase in fluorescence lifetime and anisotropy of TMR upon binding of agonist, as well as biexponential decays for both agonist-bound and ligand-free samples, suggesting conformational heterogeneity.

Figure 5 shows four ABEL-trapped ligand-free receptors exhibiting a representative range of behaviors. Fluorescence intensity (blue) and lifetime (green) are plotted on the same time axis with 10 ms bins. The most striking feature of the data is the presence of discrete intensity steps. Given these evident digital transitions, we applied a change-point algorithm[35] to statistically identify the time points during which the intensity of a trapped receptor changes significantly. For clarity, we use the word "state" to describe the microscopic conformation of the single receptor in between such change-points, as reported by the TMR dye. Although many receptors dwell in only one state before the TMR dye photobleaches (5a), in others we observe a range of state-to-state dynamics, including correlated intensity and lifetime changes (5b), uncorrelated changes (5c), and mixed behaviors (5d). By eye, we observed qualitatively similar behavior for both ligand-free and agonist-bound receptors. Moreover, we did not observe evidence for a simple "clustering" of the data into a small number of well-resolved states. Instead, the data suggest a range of conformational states in both ligand-free and agonist-bound samples. Panels 5e and 5f show two-dimensional density plots (histograms) of the observed distribution of intensity-lifetime states for both ligand-free and agonist-bound receptors. A change is evident: ligand-free receptors populate more states at lower intensity and

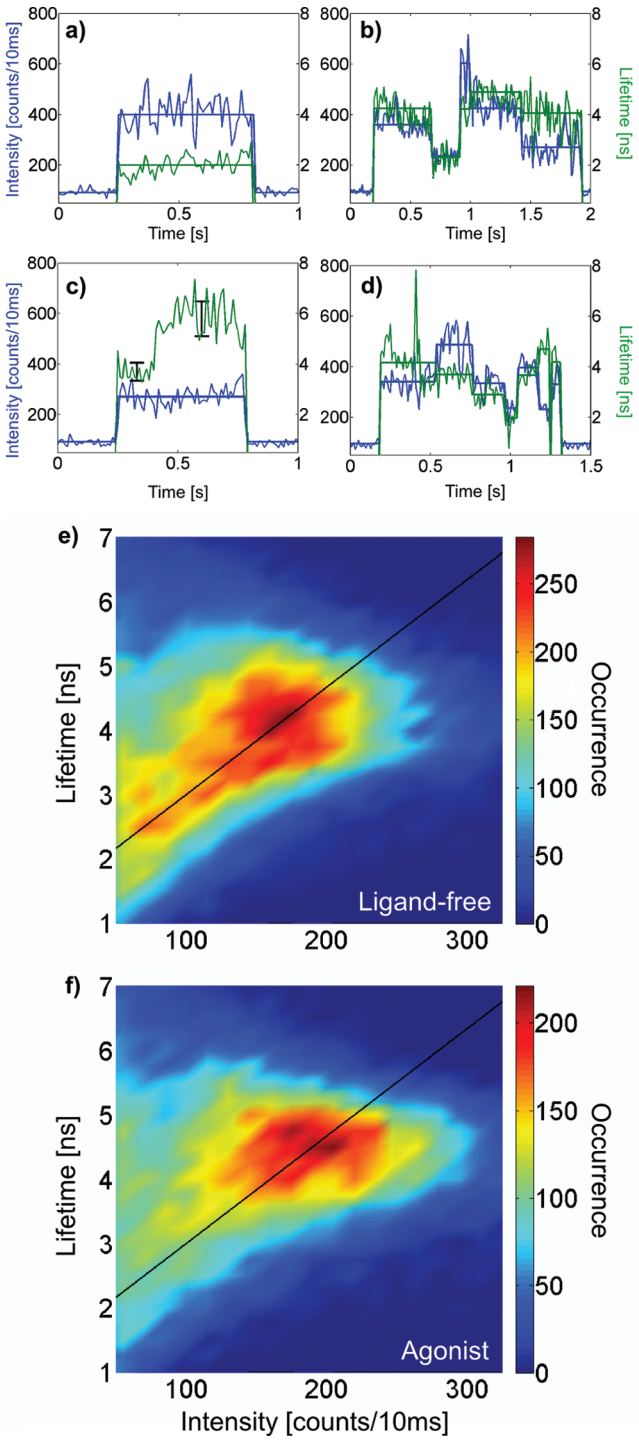

FIGURE 5. Four ABEL-trapped β_2ARs (a−d) showing discrete states in intensity (blue) and lifetime (green). Plotting the distribution of these intensity-lifetime states for many ligand-free and agonist-bound β_2ARs (e,f) allows visualization of the shift in conformational equilibria upon binding of agonist. As a guide to the eye, we plot a diagonal line to highlight states of constant radiative lifetime, $\tau_{rad} = k_{rad}^{-1} \propto \tau/I$, where τ is the fluorescence lifetime and I is the intensity of the state.

lifetime, whereas the agonist-bound receptors are more restricted to higher intensity and lifetime. The broad distribution of intensity-lifetime states indicates significant variation of radiative and nonradiative rates in TMR, reflecting conformational diversity in the receptor microenvironment.

While Figure 5 allows us to observe the systematics of intensity-lifetime states, analysis of the dwell times within each state and also the fluorescence fluctuations within states by autocorrelation methods show a clear increase in mean dwell time and slower fluctuations in the presence of agonist.[27] Taken together, our analysis allows access to fluctuation time scales in β_2AR over 3 orders of magnitude, milliseconds to seconds, which are inaccessible to other techniques.[56]

Redox Cycling of Nitrite Reductase

The ABEL trap allows measurements to be performed on single solution-phase enzymes for prolonged periods of time without immobilization or encapsulation. We applied the ABEL trap to study the dynamics of nitrite reductase (NiR),[57] a multicopper enzyme that catalyzes the one-electron reduction of nitrite to nitric oxide.[58] NiR was labeled with an Atto647N fluorescent dye that is partially quenched by the enzyme's oxidized type I Cu, but is not quenched by reduced type I Cu, converting the dye into a fluorescent indicator of the redox state of a single Cu atom (Figure 6a).[59] We chose to study NiR because a dye molecule covalently bound to the enzyme provides a source of photons for the ABEL trap to use for enzyme position estimations, even in the dye's partially quenched state, and because previous measurements on single, immobilized NiR molecules showed evidence of static and dynamic heterogeneity, with the origins of this heterogeneity largely unexplored.[59]

Individual molecules of labeled NiR were trapped for multiple seconds, and intensity fluctuations, indicative of redox state shifts of the proximal type I Cu atom, were observed (Figure 6b,c).[57] Data traces were recorded under turnover conditions for a variety of substrate concentrations. A non-redox-active labeled control protein did not show such fluctuations, confirming their link to the enzyme's intrinsic redox processes. A waiting time analysis was performed, with dwell times in the bright or dark system states recorded from many individual molecules as a function of substrate concentrations. The dwell time distribution in the bright state was observed to shift to short dwell times with increasing substrate concentration, while the opposite trend was observed for the dark state. The equilibrium population ratio between light and dark state shifted to favor the dark state as substrate concentration was increased.

To model the system dynamics, we used a kinetic scheme that explicitly treats substrate binding and intramolecular

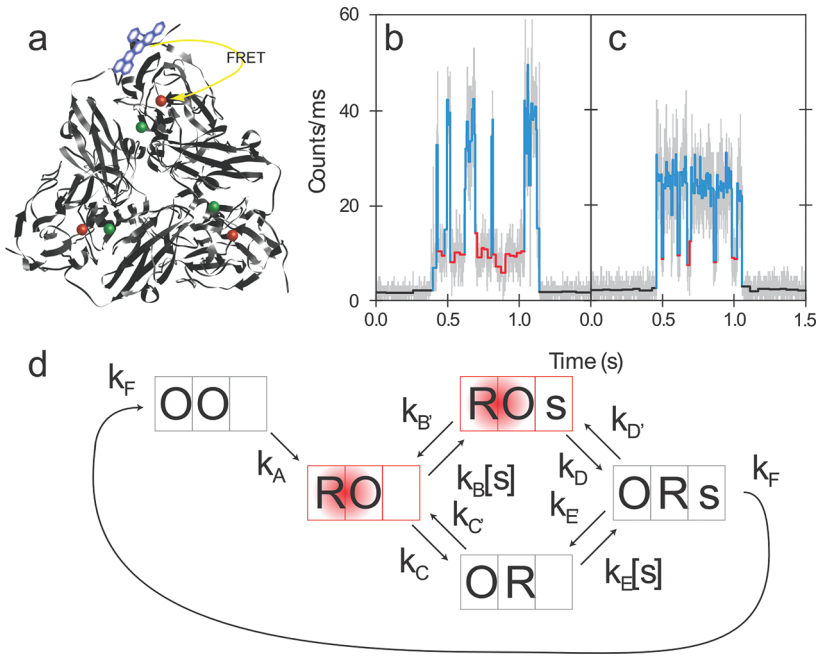

FIGURE 6. Redox cycling of blue nitrite reductase (bNiR). (a) bNiR molecules are labeled with an Atto647N dye molecule, which is a fluorescent indicator of the proximal Cu redox state. (b,c) Individual molecules of solution-phase bNiR fluctuate between two digital intensity levels, corresponding to the oxidized (red) and reduced (blue) Cu redox states. (d) Dwell time distributions in the oxidized and reduced states were fit to a kinetic model, where R/O – R/O – s/null in the boxes represent the redox state of the type I Cu (reduced/oxidized), type II Cu (reduced/oxidized), and the presence or absence of nitrite substrate, respectively. The red boxed species correspond to the bright states. Fits to the dwell time distributions yielded all 10 rate constant parameters.

electron transfer (ET) between the type I and type II Cu atoms as distinct and chronologically independent events (Figure 6d).[57,59] Analytic forms for the expected dwell time distributions[60–62] and population ratios were determined, and a global fit was used to extract all 10 rate constants in the kinetic scheme. The dwell time in the bright state is dominated by the intramolecular ET rate and shifts in the observed distribution are largely as a result of the enzyme population shifting from a substrate-unbound state with ET rate constant, k_C, to a substrate-bound state with ET rate constant, k_D. The influence of substrate binding on the value of this ET rate constant is a current topic of considerable interest with different experimental methods yielding qualitatively different trends.[63] Use of the extracted parameters in further modeling paints a picture of protein dynamics where ordered mechanisms dominate at the extremes of substrate concentration, with substrate binding preceding ET at high substrate concentrations and following ET at low substrate concentrations, but a random-sequential mechanism dominates at intermediate concentrations. By allowing observation of the asynchronous events in bNiR's catalytic cycle, we have been able to gain a unique perspective into the dynamics of a solution-phase enzyme under turnover conditions.

Conclusions and Outlook

With the ability to counter Brownian motion, the ABEL trap has provided new insights into the photophysics, conformational dynamics, binding stoichiometry, and enzymatic cycling of a variety of biological macromolecules in aqueous buffer. We envision the ABEL trap to be even more powerful when combined with other single-molecule spectroscopy modalities such as FRET, anisotropy, fluorescence spectrum, and so forth.

The new generation of ABEL traps has added the capability of measuring diffusion coefficient and/or electrokinetic mobility of trapped objects with unprecedented precision. It might soon become possible to observe individual protein–protein interactions and binding/unbinding processes in the trap. By increasing the length of the trapping time,[30,31] additional mechanistic details will become available, for example, extraction of enzymatic rate constants on a *per molecule* basis. The examples reported here show only a few areas where the ABEL trap can be utilized to explore heterogeneous behaviors for single molecules.

We warmly thank the following current and former collaborators: N. R. Douglas, N. R. Conley, E. J. Miller, and J. Frydman (TRiC studies), A. Fürstenberg, X. J. Yao, and B.K. Kobilka (GPCR), L. C.

Tabares, D. Kostrz, C. Dennison, T. J. Aartsma, and G. W. Canters (bNiR), and A. E. Cohen (initial trap design). The authors acknowledge the Division of Chemical Sciences, Geosciences, and Biosciences, Office of Basic Energy Sciences of the U.S. Department of Energy through Grant DE-FG02-07ER15892 for funding work on antenna proteins and redox enzymes, NIH Grant No. PN2-EY-16525 for work on TRiC, and NIH Grant. No. 1R21-RR023149-03 for initial trap development.

BIOGRAPHICAL INFORMATION

Quan Wang received his B.S. in physics from University of Science and Technology of China and M.S. in Optical Science and Engineering from the University of New Mexico. He is currently a Ph.D. student at Stanford University, working with Prof. W. E. Moerner.

Randall H. Goldsmith earned his B.A. at Cornell and his Ph.D. at Northwestern with Professors Mark Ratner and Mike Wasielewski. He recently completed his postdoctoral study with Professor W. E. Moerner at Stanford, where he developed a profound appreciation for molecules as individuals. He is currently an Assistant Professor in the Department of Chemistry at the University of Wisconsin—Madison.

Yan Jiang received her B.S. degree in Fundamental Sciences (Mathematics and Physics) from Tsinghua University in 2006. She is currently a Ph.D. candidate in the Applied Physics Department, Stanford University.

Samuel D. Bockenhauer completed baccalaureate studies at the University of Wisconsin—Madison in Physics and English. Following graduation in 2007, he moved to the west coast to pursue a Physics Ph.D. at Stanford in the laboratory of W. E. Moerner.

W. E. Moerner is the Harry S. Mosher Professor of Chemistry and Professor, by courtesy, of Applied Physics at Stanford University.

FOOTNOTES

*To whom correspondence should be addressed. E-mail:wmoerner@stanford.edu. Telephone: 650-723-1727. Fax: 650-725-0259.
The authors declare no competing financial interest.
[⊥]Department of Chemistry, University of Wisconsin, Madison.

REFERENCES

1 Moerner, W. E.; Kador, L. Optical detection and spectroscopy of single molecules in a solid. *Phys. Rev. Lett.* **1989**, *62*, 2535–2538.
2 Orrit, M.; Bernard, J. Single pentacene molecules detected by fluorescence excitation in a p-terphenyl crystal. *Phys. Rev. Lett.* **1990**, *65*, 2716–2719.
3 Moerner, W. E. Single-Molecule Optical Spectroscopy and Imaging: From Early Steps to Recent Advances. In *Single Molecule Spectroscopy in Chemistry, Physics and Biology: Nobel Symposium 138 Proceedings*; Gräslund, A., Rigler, R. Widengren, J., Eds.; Springer Series in Chemical Physics 96, Springer-Verlag: Berlin, 2010; pp 25−60.
4 Ha, T. Structural Dynamics and Processing of Nucleic Acids Revealed by Single-Molecule Spectroscopy. *Biochemistry* **2004**, *43*, 4055–4063.
5 Yang, H.; Luo, G.; Karnchanaphanurach, P.; Louie, T.; Rech, I.; Cova, S.; Xun, L.; Xie, X. S. Protein conformational dynamics probed by single-molecule electron transfer. *Science* **2003**, *302*, 262–266.
6 English, B. P.; Min, W.; van Oijen, A. M.; Lee, K. T.; Luo, G.; Sun, H.; Cherayil, B. J.; Kou, S. C.; Xie, X. S. Ever-fluctuating single enzyme molecules: Michaelis-Menten equation revisited. *Nat. Chem. Biol.* **2006**, *2*, 87–94.
7 Smiley, R. D.; Hammes, G. G. Single molecule studies of enzyme mechanisms. *Chem. Rev.* **2006**, *106*, 3080–3094.
8 Yildiz, A.; Forkey, J. N.; McKinner, S. A.; Ha, T.; Goldman, Y. E.; Selvin, P. R. Myosin V walks hand-over-hand: Single fluorophore imaging with 1.5-nm localization. *Science* **2003**, *300*, 2061–2065.
9 Weiss, S. Fluorescence Spectroscopy of Single Biomolecules. *Science* **1999**, *283*, 1676–1683.
10 Joo, C.; Balci, H.; Ishitsuka, Y.; Buranachai, C.; Ha, T. Advances in Single-Molecule Fluorescence Methods for Molecular Biology. *Annu. Rev. Biochem.* **2008**, *77*, 51–76.
11 Moerner, W. E. New directions in single-molecule imaging and analysis. *Proc. Natl. Acad. Sci. U.S.A.* **2007**, *104*, 12596–12602.
12 See examples in *Single Molecule Spectroscopy in Chemistry, Physics and Biology, Nobel Symposium 138 Proceedings*; Gräslund, A., Rigler, R. Widengren, J., Eds.; Springer Series in Chemical Physics 96, Springer-Verlag: Berlin, 2010.
13 Nie, S.; Zare, R. N. Optical detection of single molecules. *Annu. Rev. Biophys. Biomol. Struct.* **1997**, *26*, 567–596.
14 Schwille, P. Fluorescence correlation spectroscopy and its potential for intracellular applications. *Cell Biochem. Biophys.* **2001**, *34*, 383–408.
15 Hess, S. T.; Huang, S.; Heikal, A. A.; Webb, W. W. Biological and chemical applications of fluorescence correlation spectroscopy: a review. *Biochemistry* **2002**, *41*, 697–705.
16 Chen, Y.; Müller, J. D.; So, P. T.; Gratton, E. The photon counting histogram in fluorescence fluctuation spectroscopy. *Biophys. J.* **1999**, *77*, 553–567.
17 Rasnik, I.; McKinney, S. A.; Ha, T. Surfaces and Orientations: Much to FRET About? *Acc. Chem. Res.* **2005**, *38*, 542–548.
18 Friedel, M.; Baumketner, A.; Shea, J. E. Effects of surface tethering on protein folding mechanisms. *Proc. Natl. Acad. Sci. U.S.A.* **2006**, *103*, 8396–8401.
19 Cohen, A. E.; Moerner, W. E. Method for trapping and manipulating nanoscale objects in solution. *Appl. Phys. Lett.* **2005**, *86*, 093109.
20 Cohen, A. E.; Moerner, W. E. Controlling Brownian motion of single protein molecules and single fluorophores in aqueous buffer. *Opt. Express* **2008**, *16*, 6941–6956.
21 Cohen, A. E.; Moerner, W. E. The Anti-Brownian ELectrophoretic trap (ABEL trap): fabrication and software. *Proc. SPIE* **2005**, *5699*, 296–305.
22 Cohen, A. E.; Moerner, W. E. Suppressing Brownian motion of individual biomolecules in solution. *Proc. Natl. Acad. Sci. U.S.A.* **2006**, *103*, 4362–4365.
23 Enderlein, J. Tracking of fluorescent molecules diffusing within membranes. *Appl. Phys. B: Laser Opt.* **2000**, *71*, 773–777.
24 Levi, V.; Ruan, Q. Q.; Gratton, E. 3-D particle tracking in a two-photon microscope: application to the study of molecular dynamics in cells. *Biophys. J.* **2005**, *88*, 2919–2928.
25 Berglund, A. J.; McHale, K.; Mabuchi, H. Feedback localization of freely diffusing fluorescent particles near the optical shot-noise limit. *Opt. Lett.* **2007**, *32*, 145–147.
26 McHale, K.; Berglund, A. J.; Mabuchi, H. Quantum dot photon statistics measured by three-dimensional particle tracking. *Nano Lett.* **2007**, *7*, 3535–3539.
27 Bockenhauer, S.; Fuerstenberg, A.; Yao, J. Y.; Kobilka, B. K.; Moerner, W. E. Conformational dynamics of single G protein-coupled receptors in solution. *J. Phys. Chem. B* **2011**, *115*, 13328–13338.
28 Wang, Q.; Moerner, W. E. Optimal strategy for trapping single fluorescent molecules in solution using the ABEL trap. *Appl. Phys. B: Laser Opt.* **2010**, *99*, 23–30.
29 Fields, A. P.; Cohen, A. E. Anti-Brownian traps for studies on single molecules. *Methods Enzymol.* **2010**, *475*, 149–174.
30 Wang, Q.; Moerner, W. E. An adaptive Anti-Brownian ELectrokinetic (ABEL) trap with real-time information on single-molecule diffusivity and mobility. *ACS Nano* **2011**, *5*, 5792–5799.
31 Fields, A. P.; Cohen, A. E. Electrokinetic trapping at the one nanometer limit. *Proc. Natl. Acad. Sci. U.S.A.* **2011**, *108*, 8937–8942.
32 Blankenship, R. E. *Molecular Mechanisms of Photosynthesis*; Blackwell Science: Oxford, 2002.
33 MacColl, R. Allophycocyanin and energy transfer. *Biochim. Biophys. Acta* **2004**, *1657*, 73–81.
34 Goldsmith, R. H.; Moerner, W. E. Watching conformational- and photodynamics of single fluorescent proteins in solution. *Nat. Chem.* **2010**, *2*, 179–186.
35 Watkins, L. P.; Yang, H. Detection of intensity change points in time-resolved single-molecule measurements. *J. Phys. Chem. B* **2005**, *109*, 617–628.
36 Loos, D.; Cotlet, M.; De Schryver, F. C.; Habuchi, S.; Hofkens, J. Single-molecule spectroscopy selectively probes donor and acceptor chromophores in the phycobiliprotein allophycocyanin. *Biophys. J.* **2004**, *87*, 2598–2608.
37 Ying, L.; Xie, X. S. Fluorescence spectroscopy, exciton dynamics, and photochemistry of single allophycocyanin trimers. *J. Phys. Chem. B* **1998**, *102*, 10399–10409.
38 Rothwell, P. J.; Berger, S.; Kensch, O.; Felekyan, S.; Antonik, M.; Wohrl, B. M.; Restle, T.; Goody, R. S.; Seidel, C. A. Multiparameter single-molecule fluorescence spectroscopy reveals heterogeneity of HIV-1 reverse transcriptase:primer/template complexes. *Proc. Natl. Acad. Sci. U.S.A.* **2003**, *100*, 1655–1660.
39 Lampa-Pastirk, S.; Beck, W. F. Intramolecular vibrational preparation of the unfolding transition state of Zn^{II}-substituted cytochrome c. *J. Phys. Chem. B* **2006**, *110*, 22971–22974.
40 Vallee, R. A. L.; Tomczak, N.; Kuipers, L.; Vancso, G. J.; van Hulst, N. F. Single molecule lifetime fluctuations reveal segmental dynamics in polymers. *Phys. Rev. Lett.* **2003**, *91*, 38301–1.

41 Adair, G. S.; Bock, A. V.; Field, H. J. The hemoglobin system: VI. the oxygen dissociation curve of hemoglobin. *J. Biol. Chem.* **1925**, *63*, 529–545.

42 Monod, J.; Wyman, J.; Changeux, J. P. On the nature of allosteric transitions: a plausible model. *J. Mol. Biol.* **1965**, *12*, 88–118.

43 Koshland, D. E. J.; Némethy, G.; Filme, D. Comparison of experimental binding data and theoretical models in proteins containing subunits. *Biochemistry* **1966**, *5*, 365–385.

44 Kinosita, K., Jr.; Adachi, K.; Itoh, H. Rotation of F1-ATPase: how an ATP-driven molecular machine may work. *Annu. Rev. Biophys. Biomol. Struct.* **2004**, *33*, 245–268.

45 Jiang, Y.; Douglas, N. R.; Conley, N. R.; Miller, E. J.; Frydman, J.; Moerner, W. E. Sensing cooperativity in ATP hydrolysis for single multi-subunit enzymes in solution. *Proc. Natl. Acad. Sci. U.S.A.* **2011**, *108*, 16962–16967.

46 Frydman, J. Folding of newly translated proteins in vivo: the role of molecular chaperones. *Annu. Rev. Biochem.* **2001**, *70*, 603–647.

47 Meyer, A. S.; Gillespie, J. R.; Walther, D.; Millet, I. S.; Doniach, S.; Frydman, J. Closing the folding chamber of the eukaryotic chaperonin requires the transition state of ATP hydrolysis. *Cell* **2003**, *113*, 369–381.

48 Kafri, G.; Horovitz, A. Transient kinetic analysis of ATP-induced allosteric transitions in the eukaryotic chaperonin containing TCP-1. *J. Mol. Biol.* **2003**, *326*, 981–987.

49 Reissmann, S.; Parnot, C.; Booth, C. R.; Chiu, W.; Frydman, J. Essential function of the built-in lid in the allosteric regulation of eukaryotic and archaeal chaperonins. *Nat. Struct. Mol. Biol.* **2007**, *14*, 432–440.

50 Boudjellaba, H.; MacGibbon, B.; Sawyer, P. On exact inference for change in a Poisson sequence. *Communications in Statistics - Theory and Methods* **2001**, 407–434.

51 Bockenhauer, S.; Fuerstenberg, A.; Yao, J. Y.; Kobilka, B. K.; Moerner, W. E. Anti-Brownian ELectrokinetic (ABEL) Trapping of Single β2-Adrenergic Receptors in the Absence and Presence of Agonist. *Proc. SPIE* **2012**, *8228*, 822805.

52 Rosenbaum, D. M.; Rasmussen, S. G. F.; Kobilka, B. K. The structure and function of G-protein-coupled receptors. *Nature* **2009**, *459*, 356–363.

53 Park, P. S. H.; Lodowski, D. T.; Palczewski, K. Activation of G protein-coupled receptors: Beyond two-state models and tertiary conformational changes. *Annu. Rev. Pharmacol. Toxicol.* **2008**, *48*, 107–141.

54 Swaminath, G.; Xiang, Y.; Lee, T. W.; Steenhuis, J. J.; Parnot, C.; Kobilka, B. K. Sequential binding of agonists to the beta-2-adrenoreceptor. *J. Biol. Chem.* **2004**, *279*, 686–691.

55 Rosenbaum, D. M.; Zhang, C.; Lyons, J. A.; Holl, R.; Aragao, D.; Arlow, D. H.; Rasmussen, S. G. F.; Choi, H.; DeVree, B. T.; Sunahara, R. K.; Chae, P. S.; Gellman, S. H.; Dror, R. O.; Shaw, D. E.; Weis, W. I.; Caffrey, M.; Gmeiner, P.; Kobilka, B. K. Structure and function of an irreversible agonist-beta 2 adrenoceptor complex. *Nature* **2011**, *469*, 236–240.

56 Peleg, G.; Ghanouni, P.; Kobilka, B. K.; Zare, R. N. Single-molecule spectroscopy of the beta-2 adrenergic receptor: observation of conformational substates in a membrane protein. *Proc. Natl. Acad. Sci. U.S.A.* **2001**, *98*, 8469–8474.

57 Goldsmith, R. H.; Tabares, L. C.; Kostrz, D.; Dennison, C.; Aartsma, T. J.; Canters, G. W.; Moerner, W. E. Redox cycling and kinetic analysis of single molecules of solution-phase nitrite reductase. *Proc. Natl. Acad. Sci. U.S.A.* **2011**, *108*, 17269−17274.

58 Averill, B. A. Dissimilatory nitrite and nitric oxide reductases. *Chem. Rev.* **1996**, *96*, 2951–2964.

59 Kuznetsova, S.; Zauner, G.; Aartsma, T. J.; Engelkamp, H.; Hatzakis, N.; Rowan, A. E.; Nolte, R. J. M.; Christianen, P. C. M.; Canters, G. W. The enzyme mechanism of nitrite reductase studied at single-molecule level. *Proc. Natl. Acad. Sci. U.S.A.* **2008**, *105*, 3250–3255.

60 Van Kampen, N. G. *Stochastic Processes in Physics and Chemistry*; Elsevier: Amsterdam, 1992; pp 44−47.

61 Xie, X. S. Single-molecule approach to enzymology. *Single Mol.* **2001**, *2*, 229–236.

62 Cao, J. Event-averaged measurements of single-molecule kinetics. *Chem. Phys. Lett.* **2000**, *327*, 38–44.

63 Wijma, H. J.; Jeuken, L. J. C.; Verbeet, M. P.; Armstrong, F. A.; Canters, G. W. A random-sequential mechanism for nitrite binding and active site reduction in copper-containing nitrite reductase. *J. Biol. Chem.* **2006**, *281*, 16340–16346.